

Fabrication of nanostructure for sensing application

Mati Horprathum¹, Pitak Eiamchai¹ and Jakrapong Kaewkhao^{2,*}

¹Optical Thin-Film Laboratory National
Electronics and Computer Technology Center
Pathumthani 12120, Thailand

²Center of Excellence in Glass Technology and Materials Science
Nakhon Pathom Rajabhat University, Nakhon Pathom 73000, Thailand

Abstract

A nanostructural film is one of the highly exploiting research areas particularly in applications in sensor, photocatalytic, and solar-cell technologies. We therefore present morphological and nanostructural properties of tungsten oxide (WO_3) and aluminum oxide (Al_2O_3). In addition, we further explore engineered nanostructures which enable controls of optical, electrical, and mechanical properties. These improvements led to practical applications in gas sensors and surface-enhanced Raman.

Keywords: Nanostructure, tungsten oxide, aluminum oxide

บทคัดย่อ

การพัฒนาโครงสร้างนาโนได้รับความสนใจอย่างมาก เนื่องจากสามารถนำไปประยุกต์ใช้งานได้อย่างแพร่หลาย ทั้งในด้านอุปกรณ์ตรวจจับ ตัวเร่งปฏิกิริยาทางแสง และโซลาร์เซลล์ เป็นต้น ในงานวิจัยนี้ได้นำเสนอการพัฒนาโครงสร้างนาโนของทังสเตนไดรอกไซด์ และอะลูมิเนียมออกไซด์ ในการควบคุมสมบัติทางแสง ไฟฟ้าและทางกล โดยจากการพัฒนาโครงสร้างนาโนนี้สามารถที่จะนำไปประยุกต์ใช้เพื่อเพิ่มประสิทธิภาพของอุปกรณ์ตรวจจับแก๊ส และพื้นผิวขยายสัญญาณรามานได้

คำสำคัญ: โครงสร้างนาโน, ทังสเตนไดรอกไซด์, อะลูมิเนียมออกไซด์

1. Introduction

Recent advancements in nanostructured materials have provided significant breakthroughs in several practical applications in nanoelectronics, photonics, and bioengineering according to intrinsically unique physical and chemical properties [1-4]. The nanostructure thin films also have potential for functional devices as photonic crystals, catalysts, and sensor. Fabrications of the nanostructured thin films hence have an enormous impact on a wide variety of technological areas and research focuses. To fabricate such nanostructures, several approaches have been employed to date, including nanolithography-based [5, 6], hydrothermal [7-9] and vapor-liquid-solid (VLS) [10-12] methods. Most methods typically

require complex procedures for deposition or functionalization using liquid-based processes, or high temperature annealing and produce nanostructure with random size, distribution and orientation, which are not reliable for practical applications because of poor reproducibility. Recently, some processes including e-beam lithography, nanolithography and reactive ion etching have been developed to realize well-ordered nanostructures. Nevertheless, they either require expensive instrumentation or complicated fabrication procedures. Therefore, enhancement of sensor surface area using a simple and low cost methods for well-ordered nanostructure construction are more preferred in sensor devices would be advantageous. Alternatively, physical vapor de-

*Corresponding author; e-mail: mink110@hotmail.com

position (PVD) with glancing angle deposition (GLAD) technique [13-15] and anodic aluminum oxide (AAO) template [16] is highly potential and highly efficient for the preparation of active layer of the sensor device, because of simple process and high surface area.

In this article, we therefore explored our nanostructural fabrications of WO₃ nanorods and porous aluminum oxide materials by sputtering with the GLAD technique and anodization method respectively. We further exemplified and discussed real applications in gas sensors and surface-enhanced Raman spectroscopy (SERS).

2. Experimental detail

2.1 Fabrication of WO₃ NRs by magnetron sputtering with the GLAD Technique for gas-sensor

The WO₃ nanorods were fabricated by the DC magnetron sputtering. For the WO₃ nanorod fabrication, the substrate normal was positioned at an angle of 85° ($\alpha = 85^\circ$) with the respect to the vapor incident flux (the vertical axis) as shown in Figure 1.

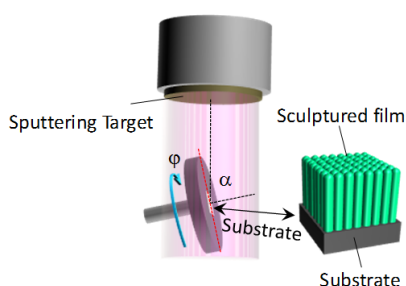


Figure 1. Schematic diagram of the sputtering system with the GLAD technique.

Tungsten of 99.995% purity was used as the sputtering target. We controlled nanorod structure by fixed glancing angle at 85°. The substrate rotation was set to 1.6 rpm. During the sputtering, the distance between the target and the substrate was 7 cm. The WO₃ nanorod films were deposited under the following deposition condition: base pressure of 7.0×10^{-6} mbar, operating pressure of 5.6×10^{-3} mbar. All samples were reactively sputtered in a mixture of 99.999% argon and 99.999% pure oxygen. The flow rate of Ar and O₂ were kept at constant value of 6.6 and 10.5, respectively. The WO₃ nanorods films were grown on p-type silicon (100) wafers and glass slides. Both of which had been sequentially cleaned

in ultrasonic washer with acetone and isopropanol, and then dried in the nitrogen atmosphere, before being loaded into the deposition chamber.

2.2 Fabrication of Porous Al₂O₃ Template by a two-step anodizing process for SERS substrate

The AAO template fabricated by a two-step anodizing process at low temperature on UHV-foil substrate, aims to increase the surface area and prevent coalescence of the deposited silver nanoparticles as shown in Figure 2. The commercial UHV aluminum foils were used as base material for the fabrication of nanoporous anodic aluminum oxide (AAO) template. These UHV-foils were cleaned by acetone and then rinsed with deionized water. Both steps were carried out in ultrasonic bath. Subsequently, electro-polished in a mixture solution of perchloric acid and ethanol at a volume ratio of 1:4. At step 1, the first anodization was carried out in 0.3 M oxalic acid for 4 h at 0°C. At the next step, the produced alumina layer was eroded in a mixture solution of phosphoric acid (6 wt. %) and chromic acid (2 wt. %) at 65°C. At the third step, the second anodization was performed with the same condition as the first, but only for 1 h. At the last step, these AAO substrates were further etched in 5% phosphoric acid at room temperature for 60 minutes in order to enlarge the diameter of the nanochannels. On the prepared AAO templates, the silver nanoparticles were deposited by the DC magnetron sputtering system. The base pressure of the vacuum chamber was first obtained at 8×10^{-7} Torr. Then, an argon sputtering gas was constantly supplied to the chamber at 20 sccm. During the deposition, operating pressure, sputtering power, and deposition time were maintained at 5 mTorr, 100 Watt, and 8 s, respectively.

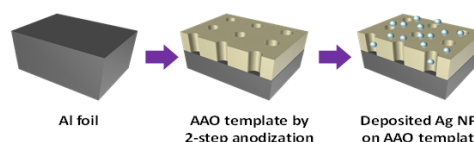


Figure 2. Schematic diagram of SERS substrate fabrication by Ag NPs deposited on AAO template.

Morphologies of the nanostructure films were all investigated by field-emission scanning electron microscopy (FE-SEM; Hitachi S-4700). The properties

suitable for practical applications will be discussed in the next section.

3. Result and discussion

3.1 WO₃ nanorods for NO₂ gas-sensor

Generally, WO₃-based metal oxide gas sensor has been extensively studied due to its high sensitivity to various gases especially nitrogen dioxide (NO₂), which is a common air pollutant produced during combustion in automotive engines and industrial factories. FE-SEM images of WO₃ nanorods and dense film were shown in Figure 3. The WO₃ deposited at conventional sputtering method ($\alpha = 0^\circ$), the results demonstrated the dense WO₃ films (Figure 3(a)). When the angle was 85° (Figure 3(b)), the shadowing effect dominated the growth process and the columnar film formations were produced.

We successfully fabricated the WO₃ nanorods for improved NO₂-gas sensing applications compare with dense WO₃ films as show in Figure 4. The results clearly show that the WO₃ nanorods yielded much improved performance due to much larger effective surface area [13, 15].

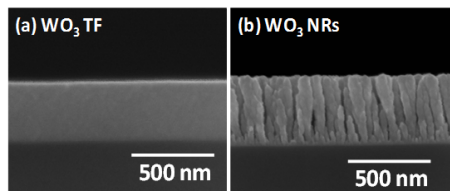


Figure 3. Cross-sectional FE-SEM images of the nanostructure WO₃ films prepared by the (a) conventional sputtering deposition and (b) GLAD techniques.

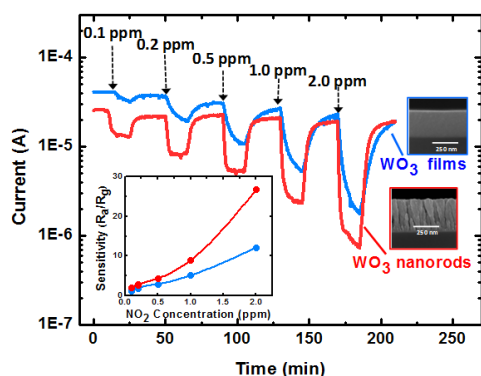


Figure 4. Dynamic responses of NO₂ gas sensors based on the WO₃ (a) films, and (b) nanorods at 250°C operating temperature.

3.2 Ag nanoparticle decorated on AAO template for SERS application

Recently, SERS has attracted an increased attention to the investigations of various chemical reactions on metal surfaces. A critical aspect of SERS-related applications is to develop a specific morphology of the metal surfaces to alter the local electric field and achieve a reproducible and high level of enhancement. Figure 5 shows the top-view FE-SEM images of three types of the SERS substrates were used in this experiment. From Figure 5(a), the fabricated AAO template was observed at approximately 80 nm in diameter and 110 nm in interporous distances. Figure 5(b) shows the AgNPs sputtered on the bare silicon wafer. From Figure 5(c), the 3D-hybrid SERS substrate was prepared with the decoration of the AgNPs on the AAO template. Although the deposition time of the AgNPs were the same in Figure 5(b) and (c), we instead observed the AgNPs' average diameter at approximately 5 nm on the AAO template.

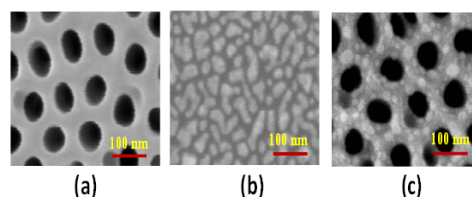


Figure 5. Top-view FE-SEM images of the different SERS substrates: (a) the AAO template, (b) the AgNPs on the Si wafer, and (c) the AgNPs decorated on AAO template.

With the AAO template, the authors deposited Ag nanoparticle on AAO template as the SERS substrates, whose enhancement factors highly depended on their physical morphology. These three types of the SERS substrates were consequently examined for the SERS activities with the MB molecules. After the MB droplets on each substrates dried out, the Raman spectra were collected and plotted. Figure 6 clearly proved that the Ag nanoparticle decorated on AAO template had stronger Raman enhancement than the pure AAO template and the AgNPs on the Si wafer. The results therefore suggested that the AAO template played a significant role in preventing a coalescence of the AgNPs on the surface of the AAO template. With the relatively small size of the AgNPs, the hot spots still remained

at particle junctions despite significant necking, resulting in exhibited excellent SERS on the AAO template than on the Si substrate.

4. Conclusion

We presented the recent status in the investigations of the nanostructured films fabricated by the sputtering deposition with GLAD technique and anodization process toward practical applications. We successfully fabricated nanomaterials WO_3 nanorods and Al_2O_3 nanoporous. In addition, three-dimensional nanostructure could result in more novel applications in the field of gas-sensors and SERS.

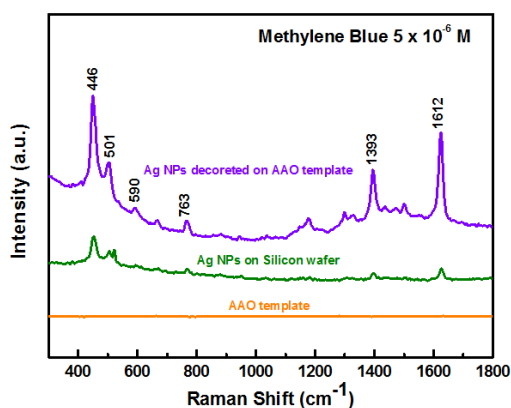


Figure 6. The Raman signals of the 5×10^{-6} M methylene blue droplets on the different SERS substrates.

References

- [1] Steele, J. J. & Brett, M. J. (2007). *J. Mater. Sci: Mater Electron.*, 18, 367-379.
- [2] Hawkeye, M. M. & Brett, M. J. (2007). *J. Vac. Sci. Technol.*, A 25, 1317-1335.
- [3] Steele, J. J., Taschuk, M. T., & Brett, M. J. (2008). *IEEE Sens. J.*, 8, 1422-1429.
- [4] Zhao, Y. P., Ye, D. X., Wang, G. C., & Lu, T. M. (2003). Designing nanostructures by glancing angle deposition. *SPIE Proceedings*, 5219, 59-73.
- [5] Zhao, X. M., Xia, Y., & Whitesides, G. M. (1997). *J. Mater. Chem.*, 7 (7), 1069-1074.
- [6] Hulteen, J. C. & Van Duyne, R. P. (1995). *J. Vac. Sci. Technol.*, A 13 (3), 1553-1558.
- [7] Khamkhom, P., Horprathum, M., Eiamchai, P., Chananonawathorn, C., & Kaewkhao, J. (2014). Investigation on nanostructure and morphologies of ZnO nanowires prepared by hydrothermal method. *Advanced Materials Research*, 979, 192-195.
- [8] Limnonthakul, P., Chananonawathorn, C., Aiempnanakit, K., Kaewkhao, J., Eiamchai, P., & Horprathum, M. (2013). Effects of precursor concentration on Hexagonal structures of ZnO nanorods grown by aqueous solution method. *Advanced Materials Research*, 770, 120-123.
- [9] Kalasung, S., Chananonawathorn, C., Horprathum, M., Thongpanit, P., Eiamchai, P., Limwichean, S., Pattanaboonmee, N., Witit-Anun, N., & Aiempnanakit, K. (2013). Low-temperature synthesis of nanocrystalline ZnO nanorods arrays. *Advanced Materials Research*, 770, 237-240.
- [10] Nagashima, K., Yanagida, T., Kanai, M., Oka, K., Klamchuen, A., Rahong, S., Meng, G., Horprathum, M., Xu, B., Zhuge, F.W., He, Y., & Kawai, T. (2012). Switching properties of titanium dioxide nanowire memristor. *Jpn. J. Appl. Phys.*, 51, 11PE09.
- [11] Klamchuen, A., Yanagida, T., Kanai, M., Nagashima, K., Oka, K., Rahong, S., Gang, M., Horprathum, M., Suzuki, M., Hidaka, Y., Kai, S., & Kawai, T. (2011). Study on transport pathway in oxide nanowire growth by using spacing-controlled regular array. *Appl. Phys. Lett.*, 99, 193105.
- [12] Nagashima, K., Yanagida, T., Oka, K., Kanai, M., Klamchuen, A., Rahong, S., Meng, G., Horprathum, M., Xu, B., Zhuge, F., He, Y., Park, B. H., & Kawai, T. (2012). *Nano Lett.*, 12 (11), 5684-5690.
- [13] Horprathum, M., Limwichean, K., Wisitsoraat, A., Eiamchai, P., Aiempnanakit, K., Limnonthakul, P., Nuntawong, N., Pattantsetakul, V., Tuantranont, A., & Chindaudom, P. (2013). NO_2 -sensing properties of WO_3 nanorods prepared by glancing angle DC magnetron sputtering. *Sensors and Actuators B: Chemical*, 176, 685-691.

- [14] Wongchoosuk, C., Wisitsoraat, A., Phokharatkul, D., Horprathum, M., Tuantranont, A., & Kerdcharoen, T. (2013). Carbon doped tungsten oxide nanorods NO₂ sensor prepared by glancing angle RF sputtering. **Sensors and Actuators B: Chemical**, 181, 388-394.
- [15] Srichaiyaperk, T., Aimpanakit, K., Horprathum, M., Limwichean, S., Chananonnawathorn, C., Wisitsoraat, A., Samransuksamer, B., Phokharatkul, D., Eiamchai, P., & Chindaudom, P. (2013). Preparation of WO₃ nanorods by glancing angle DC reactive magnetron sputtering deposition for NO₂ gas sensing application. **Advanced Materials Research**, 770, 267-270.
- [16] Nuntawong, N., Horprathum, M., Eiamchai, P., Wong-ek, K., Patthanasettakul, V., & Chindaudom, P. (2010). Surface-enhanced Raman scattering substrate of silver nanoparticles depositing on AAO template fabricated by magnetron sputtering. **Vacuum**, 84, 1415-1418.